Testing for Markovian character and modeling of intermittency in solar wind turbulence

Marek Strumik*
Space Research Centre, Polish Academy of Sciences, Bartycka 18 A, 00-716 Warsaw, Poland

Wiesław M. Macek
Faculty of Mathematics and Natural Sciences, College of Sciences, Cardinal Stefan Wyszyński University, Dewajtis 5, 01-815 Warsaw, Poland
and Space Research Centre, Polish Academy of Sciences, Bartycka 18 A, 00-716 Warsaw, Poland

(Received 25 June 2007; revised manuscript received 26 May 2008; published 25 August 2008)

We present results of statistical analysis of solar wind turbulence using an approach based on the theory of Markov processes. It is shown that the Chapman-Kolmogorov equation is approximately satisfied for the turbulent cascade. We evaluate the first two Kramers-Moyal coefficients from experimental data and show that the solution of the resulting Fokker-Planck equation agrees well with experimental probability distributions. Our analysis provides evidence that the transfer of fluctuations from large to smaller eddies must be independent of the dynamics on large scales and in particular it must be independent of the driving mechanisms for solar wind turbulence. Our results also suggest the presence of a local transfer mechanism for magnetic field fluctuations in solar wind turbulence.

DOI: 10.1103/PhysRevE.78.026414 PACS number(s): 96.50.Tf, 96.60.Vg, 02.50.Ga, 05.10.Gg

I. INTRODUCTION

Irregular dynamics of the solar-wind plasma exhibits many similarities to fully developed hydrodynamic turbulence. Numerous *in situ* measurements of temporal variability of parameters of the plasma have shown that their spectral distributions usually have power-law character [1–4]. Investigations of the fluctuations have also revealed their non-Gaussian probability distributions at small scales, which is commonly attributed to the intermittency phenomenon [5–8]. In fact, the solar wind provides a unique laboratory for studying high-Reynolds-number magnetohydrodynamic turbulence (see, e.g., Refs. [2,9] for reviews).

One of the main problems in the studies of incompressible hydrodynamical turbulence is explaining the statistics of velocity fluctuations on different length scales. In magnetohydrodynamic turbulence this problem concerns in general also magnetic field and density fluctuations. Conventionally, in investigations of a turbulent cascade, statistical properties of fluctuations $\delta u_\tau(t)=u(t+\tau)-u(t)$ of a physical quantity $u(t)$ are examined, where τ is the temporal (or spatial) scale. The fluctuations are studied by examining their probability distribution functions (PDFs) $P(\delta u_\tau(t))$ or n-order moments $\langle \delta u_\tau(t)^n \rangle$ of the distributions, also called structure functions. Often, if the root mean square of velocity fluctuations is small as compared to the mean velocity of the flow, one can use the Taylor hypothesis, interpreting the temporal variation δu_τ at a fixed position as a spatial variation δu_l, where l is a spatial scale corresponding to the temporal scale τ. In an intermittent turbulent cascade, the PDF of the fluctuations is non-Gaussian at small scales. When we go to larger scales, the shape of the PDF changes, and finally there is a scale τ_G, such that for $\tau > \tau_G$ the PDF is close to a Gaussian distribution [10,11].

A number of models for the scaling exponents and scaling of the probability distributions of the fluctuations have been proposed. Many papers have also been devoted to experimental verification of the proposed models (see, e.g., Refs. [9–11] for reviews). Recently, a great deal of attention has been devoted to investigations of the fluctuations in hydrodynamic turbulence from the point of view of the Markov processes theory (see, e.g., Refs. [12–17]). In particular, results of the verification of the validity of the Chapman-Kolmogorov equation as well as estimations of the Kramers-Moyal coefficients from experimental data suggest that the Markov processes approach may be appropriate to the description and modeling of the turbulent cascade [13,14,16]. The estimations of the Kramers-Moyal coefficients allow one to determine the form of the Fokker-Planck equation governing the evolution of the probability distribution with scale for the fluctuations. A model based on a Fokker-Planck equation has been recently proposed for solar wind turbulence, but for fluctuations of quantities that exhibit self-similar scaling [18]. In the present paper, the Markov processes approach has been applied to analysis of intermittent solar wind turbulence. This approach seems to provide a contact point between the pure statistics and dynamical systems approach to turbulence.

II. DATA SET

In the plasma flow expanding from the Sun into interplanetary space we can distinguish several forms, in particular the slow ($<$450 km/s) and fast ($>$600 km/s) solar wind (see, e.g., Ref. [19] and references therein). At the solar minimum the two forms are usually well separated; the fast wind is more homogeneous and incompressible in comparison with the slow wind.

Our goal here is to study properties of the turbulent cascade, therefore we try to exclude effects associated with nonstationary driving and spatial inhomogeneity of the turbu-

*maro@cbk.waw.pl

lence. For this reason, in this paper we have chosen for analysis the fast solar wind flowing from nonactive high-latitude regions in the solar corona at the solar minimum. This data set represents dynamics of the fast solar wind free of dynamical interaction with the slow wind, as possibly the most homogeneous and probably also most stationary case. Therefore effects associated with nonstationary driving should be eliminated here to a large extent, and we should observe a state possibly closest to freely decaying turbulence, which seems to be the most appropriate case to study the turbulent cascade. Since we would like to examine fluctuations in a wide range of scales, including small scales, we focus here on magnetic field fluctuations, which are available at much better time resolution in comparison with measurements of plasma parameters (e.g., bulk velocity or density of the plasma). However, we are aware of the importance of the detailed analysis of other types of the solar wind, as well as other plasma parameters, and we are going to carry out such studies in the future.

We analyze here time series obtained by the Ulysses spacecraft [20]. The magnetic field is measured by two independent triaxial sensors of the Ulysses spacecraft: a vector helium magnetometer (VHM) and a fluxgate magnetometer (FGM). These two magnetometers are located on a radial boom of the Ulysses spacecraft: the VHM sensor at the end of the 5 m boom and the FGM sensor at 1.2 m inboard from the VHM. The magnetometers use different physical principles to measure three orthogonal components of the interplanetary magnetic field vector. The VHM sensor measurements are based on the effect of the influence of an ambient magnetic field on the efficiency of optical pumping of a metastable population of He gas [21,22]. The FGM sensor uses the classical technique of measuring external magnetic fields by comparison of drive-coil currents needed to saturate the cores in opposite directions [21,23].

This dual-magnetometer measurement technique gives the possibility of detecting any background field caused by the spacecraft devices, as well as provides a way of evaluating the self-consistency of the measurements made by the two sensors. The magnetometers have been designed, built, and extensively tested to have adequate sensitivity and sufficiently low intrinsic noise to measure the interplanetary magnetic fields. Overall, with all implemented corrections, the two sensors are intercalibrated to better than 0.1 nT. In this paper we use time series based on the VHM sensor measurements prepared and provided by the Ulysses Magnetic Field Investigation Team, whereas the FGM sensor data were only used to assess the quality of the VHM measurements. A detailed description of the experimental setup and data acquisition process can be found in Ref. [21].

The data set analyzed here consists of about 1.3×10^7 measurements of the radial (the Sun-spacecraft axis) component B_R of the magnetic field obtained by the Ulysses spacecraft from 70:1996 to 230:1996 (day of year:year) at a time resolution of one second. The measurements have been obtained at heliospheric latitudes from 29 to 44 degrees and at radial distance from the Sun from 3.5 to 4.2 AU. Small gaps (up to three missing points) in the data set have been filled using linear interpolation. Further in this paper we consider fluctuations of the radial component of the magnetic field

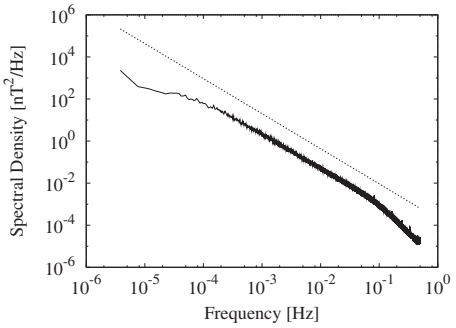

FIG. 1. Power spectrum of the radial component of the solar-wind magnetic field (solid line). The dashed line shows the spectrum of the type $E(f)\propto f^{-5/3}$ for comparison.

defined as $b(t)=B_R(t+\tau)-B_R(t)$. Presenting our results we use here temporal scales and do not recast the fluctuations into the space domain using the Taylor hypothesis. However, since we analyze highly supersonic and super-Alfvénic flow (mean velocity $U\approx744$ km/s in the reference system moving with the measuring instrument), the temporal scales physically should be interpreted rather as spatial scales. Assuming that the Taylor hypothesis is satisfied here, one can easily transform the temporal scale τ to the spatial scale l using the relationship $l=U\tau$ [10]. However, in general it is not possible to distinguish between temporal and spatial variations in the case of one-point measurements of plasma parameters, as it is for the Ulysses spacecraft.

In Fig. 1 we show the power spectrum of the radial component of the magnetic field. As one can see, the power spectrum has a power-law character with the spectral exponent very close to $-5/3$ in the inertial range identified here as stretching approximately from 0.0002 to 0.075 Hz.

III. MARKOV PROCESSES APPROACH

We investigate here statistics of fluctuations $b(t)=B_i(t+\tau)-B_i(t)$ of a component $B_i(t+\tau)$ of the magnetic field at a scale τ. We consider the fluctuations as a stochastic process in scale, i.e., we assume that a turbulent cascade is responsible for the transfer of a fluctuation b_i at the largest (energy-containing) scale τ_i to a fluctuation b_{i-1} at a smaller scale τ_{i-1}, then the fluctuation b_{i-1} at the scale τ_{i-1} to a fluctuation b_{i-2} at a scale τ_{i-2}, and so forth until the dissipation scale is reached. Using the joint probability density $P(b_1,\tau_1;b_2,\tau_2)$ of finding the fluctuations b_1 at a scale τ_1 and b_2 at a scale τ_2, where $\tau_1<\tau_2$, we can define the conditional PDF as

$$P(b_1,\tau_1|b_2,\tau_2)=\frac{P(b_1,\tau_1;b_2,\tau_2)}{P(b_2,\tau_2)}. \tag{1}$$

By analogy to the definition of the two-point probability distributions, we can define the joint and conditional probability densities for longer sequences of fluctuations $b_1,b_2,b_3,\ldots$ at scales $\tau_1,\tau_2,\tau_3,\ldots$. In the case of a Markov stochastic process, by definition the following condition must be satisfied:

$$P(b_1,\tau_1|b_2,\tau_2;\ldots;b_N,\tau_N)=P(b_1,\tau_1|b_2,\tau_2), \tag{2}$$

thus the N-point joint PDF $P(b_1,\tau_1;b_2,\tau_2;\ldots;b_N,\tau_N)$ is determined by the product of conditional probabilities $P(b_{i-1},\tau_{i-1}|b_i,\tau_i)$, where $\tau_{i-1}<\tau_i$. A physical interpretation of the Markov property expressed by Eq. (2) is that a given stochastic process is "memoryless," i.e., the most recent conditioning determines completely the probability of transition from the present to the next state of the stochastic process.

For a finite set of experimental data, the Markov property can be verified by comparison of a conditional PDF $P_{\mathrm{E}}(b_1,\tau_1|b_2,\tau_2)$ evaluated directly from data with the PDF computed using the Chapman-Kolmogorov equation

$$P(b_1,\tau_1|b_2,\tau_2)=\int_{-\infty}^{\infty}P(b_1,\tau_1|b',\tau')P(b',\tau'|b_2,\tau_2)db', \tag{3}$$

where $\tau_1<\tau'<\tau_2$. Equation (3) is a necessary condition for a stochastic process to be Markovian. The Chapman-Kolmogorov equation can be written in a differential form using the so-called Kramers-Moyal expansion

$$-\tau\frac{\partial P(b,\tau|b_0,\tau_0)}{\partial\tau}=\sum_{k=1}^{\infty}\left(-\frac{\partial}{\partial b}\right)^k D^{(k)}(b,\tau)P(b,\tau|b_0,\tau_0). \tag{4}$$

Kramers-Moyal coefficients $D^{(k)}(b,\tau)$ can be evaluated as the limit $\Delta\tau\to 0$ of the conditional moments $M^{(k)}(b,\tau,\Delta\tau)$, namely,

$$D^{(k)}(b,\tau)=\lim_{\Delta\tau\to 0}M^{(k)}(b,\tau,\Delta\tau) \tag{5}$$

and

$$M^{(k)}(b,\tau,\Delta\tau)=\frac{\tau}{k!\Delta\tau}\int_{-\infty}^{\infty}(b'-b)^k P(b',\tau'|b,\tau)db', \tag{6}$$

where $\Delta\tau=\tau-\tau'$. If $D^{(4)}(b,\tau)=0$ then according to the Pawula theorem $D^{(k)}(b,\tau)=0$ for $k\geqslant 3$ [24]. In this case, starting from Eq. (4) we arrive at the Fokker-Planck equation

$$-\tau\frac{\partial P(b,\tau)}{\partial\tau}=\left(-\frac{\partial D^{(1)}(b,\tau)}{\partial b}+\frac{\partial^2 D^{(2)}(b,\tau)}{\partial b^2}\right)P(b,\tau), \tag{7}$$

which determines the evolution of the probability distribution function of a stochastic process generated by the Langevin equation (using Ito definition)

$$-\tau\frac{db}{d\tau}=D^{(1)}(b,\tau)+\sqrt{D^{(2)}(b,\tau)}\Gamma(\tau), \tag{8}$$

where $\Gamma(\tau)$ is the delta-correlated Gaussian noise. In comparison with the definition used in Ref. [24], the Kramers-Moyal coefficients given here are multiplied by τ, which is equivalent to a logarithmic length scale [16].

If Eq. (3) is satisfied, then the transition probability from scale τ_2 to τ_1 can be divided into transitions from τ_2 to τ' and then from τ' to τ_1. Therefore, in the case of a turbulent cascade, fulfillment of the Chapman-Kolmogorov equation for all triplets $\tau_1<\tau'<\tau_2$ in the inertial range suggests the presence of a local transfer mechanism in the cascade.

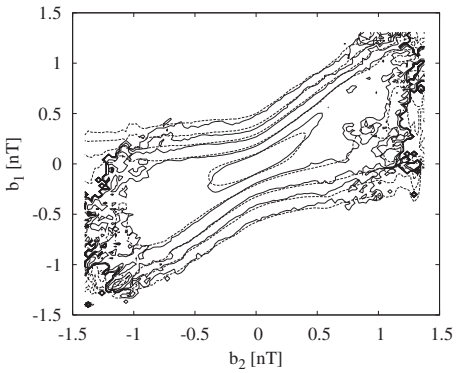

FIG. 2. Contour plots illustrating verification of the Chapman-Kolmogorov equation for $\tau_1=750$, $\tau'=1000$, and $\tau_2=1250$ s. Solid lines represent the conditional PDF $P_{\mathrm{E}}(b_1,\tau_1|b_2,\tau_2)$ evaluated directly from data, whereas dashed lines show the conditional PDF $P(b_1,\tau_1|b_2,\tau_2)$ computed using Eq. (3). The subsequent isolines correspond to the following levels of the PDF: 2.0, 0.7, 0.2, 0.07, 0.02 (from the middle of the plot).

Experimental conditional PDF $P(b_1,\tau_1|b_2,\tau_2)$ can be obtained directly from data in the following way. First, one can estimate the joint PDF $P(b_1,\tau_1;b_2,\tau_2)$ using the number of counts of different pairs (b_1,b_2) on a two-dimensional grid of bins, and apply the normalization so that the integral (appropriate sum in practice) over all bins will be equal to one. The one-dimensional PDF $P(b_2,\tau_2)$ can be estimated similarly using the one-dimensional grid of bins. Then one can compute the conditional PDF $P(b_1,\tau_1|b_2,\tau_2)$ directly from Eq. (1).

IV. RESULTS

In Fig. 2 we show superposed contour plots of the conditional PDF estimated directly from data and the PDF computed using Eq. (3) for $\tau_1=750$, $\tau'=1000$, and $\tau_2=1250$ s. One can see that corresponding contour lines for the two probability distributions are very close to each other. This indicates that the Chapman-Kolmogorov equation is (at least approximately) satisfied for the range of scales from $\tau_1=750$ to $\tau_2=1250$ s. In Fig. 3 we show the cuts through the conditional probability distributions for fixed values of b_2. As one can see, points representing cuts through

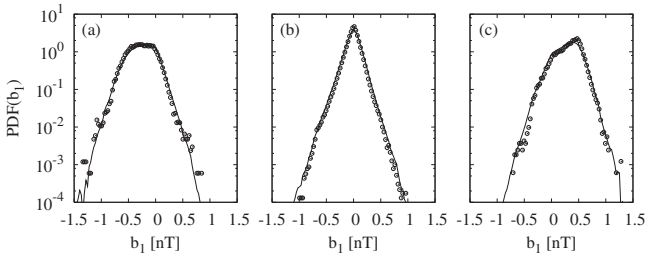

FIG. 3. Verification of the Chapman-Kolmogorov equation (3) for $\tau_1=750$, $\tau'=1000$, and $\tau_2=1250$ s. Comparisons of cuts through $P_{\mathrm{E}}(b_1,\tau_1|b_2,\tau_2)$ (points) and $P(b_1,\tau_1|b_2,\tau_2)$ (lines) from Fig. 2 are shown for fixed values of b_2, namely, (a) $b_2=-0.5$ nT, (b) $b_2=0$ nT, and (c) $b_2=0.5$ nT.

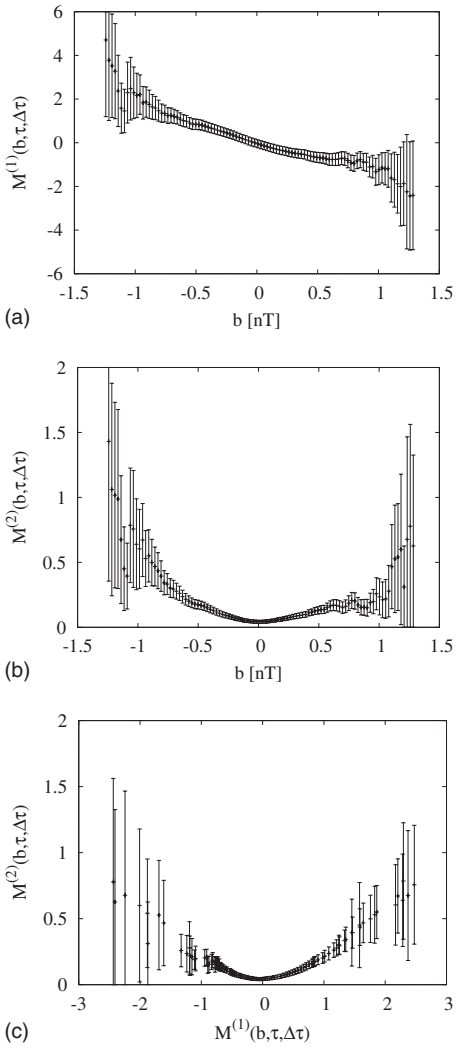

FIG. 4. The dependence of the coefficients (a) $M^{(1)}(b,\tau,\Delta\tau)$ and (b) $M^{(2)}(b,\tau,\Delta\tau)$ on b for $\tau=1000$ and $\Delta\tau=100$ s. (c) The dependence of $M^{(2)}(b,\tau,\Delta\tau)$ on $M^{(1)}(b,\tau,\Delta\tau)$.

$P_E(b_1,\tau_1|b_2,\tau_2)$ fit well to the lines representing cuts through $P(b_1,\tau_1|b_2,\tau_2)$. Repeating such a comparison for different triplets τ_1,τ',τ_2 we have checked that Eq. (3) is well satisfied in the inertial range (for scales from about 50 to 5000 s). For larger scales, outside the inertial range, the larger the scale, the worse the agreement we observe between the experimental PDF and that computed using Eq. (3). Nevertheless, Eq. (3) seems to be fulfilled up to the scale of about 24 h. Therefore, the necessary condition for Markov processes is satisfied here in the entire range of scales available for our computations, unlike in the case of hydrodynamic turbulence as reported in Ref. [16], where the cascade is not Markovian for small scales, below the Taylor length scale.

We have computed the coefficients $M^{(k)}(b,\tau,\Delta\tau)$ using the definition of Eq. (6). In Figs. 4(a) and 4(b) we present examples of the dependence of the coefficients $M^{(1)}(b,\tau,\Delta\tau)$ and $M^{(2)}(b,\tau,\Delta\tau)$ on b for $\tau=1000$ and $\Delta\tau=100$ s. In Fig. 4(c) we show the dependence of $M^{(2)}(b,\tau,\Delta\tau)$ on $M^{(1)}(b,\tau,\Delta\tau)$, which have a more regular and symmetric

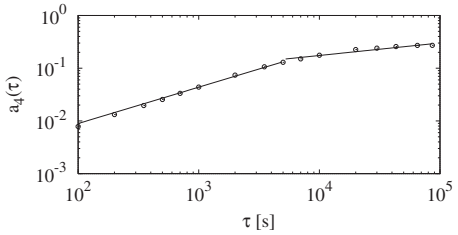

FIG. 5. Dependence of the parameter a_4 on scale τ [see Eq. (10)].

form in comparison with the dependence of $M^{(2)}(b,\tau,\Delta\tau)$ on b. We propose the following approximations: $M^{(1)}(b,\tau,\Delta\tau)=A_1(\tau,\Delta\tau)b+A_2(\tau,\Delta\tau)b^3+A_3(\tau,\Delta\tau)b^5$ and $M^{(2)}(b,\tau,\Delta\tau)=A_4(\tau,\Delta\tau)+A_5(\tau,\Delta\tau)[M^{(1)}(b,\tau,\Delta\tau)]^2$ as describing properly the experimental relationships shown in Figs. 4(a) and 4(c), correspondingly. Based on the approximations, we can fit the parameters $A_i(\tau,\Delta\tau)$ for a fixed τ and changing $\Delta\tau$, and finally compute the limits $a_i(\tau)=\lim_{\Delta\tau\to 0}A_i(\tau,\Delta\tau)$ for $i=1,\ldots,5$ (e.g., by a linear extrapolation toward $\Delta\tau=0$) obtaining the following approximations:

$$D^{(1)}(b,\tau)=a_1(\tau)b+a_2(\tau)b^3+a_3(\tau)b^5 \tag{9}$$

and

$$D^{(2)}(b,\tau)=a_4(\tau)+a_5(\tau)[D^{(1)}(b,\tau)]^2. \tag{10}$$

Repeating the entire procedure for changing τ we can also estimate the dependence of the coefficients a_i on τ. Applying the algorithm, we have obtained the following results for the inertial range ($\tau\leqslant 5000$ s): $a_1=-3.6\tau^{-0.08}$, $a_2=3.5\exp(-0.0001\tau)$, $a_3=-13.6\tau^{-0.2}$, $a_4=0.00035\tau^{0.7}$, $a_5=1.2\tau^{-0.3}$, and outside the inertial range ($\tau>5000$ s) $a_1=-0.5\tau^{0.16}$, $a_2=2$, $a_3=-2.3$, $a_4=0.016\tau^{0.26}$, $a_5=1.75\tau^{-0.36}$. As an illustration, in Fig. 5 we show the dependence of the parameter a_4 on τ. One can notice a change in the dependence for $\tau\approx 5000$ s, i.e., at the end of the inertial range.

Parametrization of $D^{(1)}(b,\tau)$ and $D^{(2)}(b,\tau)$ [shown in Eqs. (9) and (10), correspondingly] with experimentally fitted parameters $a_i(\tau)$ allows us to solve numerically Eq. (7) with initial condition taken from parametrization of the experimental PDF at a large scale τ_G, where the probability distribution of fluctuations is approximately Gaussian. Therefore we can compute numerically the PDF at scales $\tau<\tau_G$ and compare it to the experimental PDF, which allows us to verify directly our results. Such a comparison is shown in Fig. 6 for $\tau_G=86\,400$ s. As one can see there is a good agreement between experimental probability distributions and those computed from the Fokker-Planck equation.

V. DISCUSSION AND CONCLUSIONS

We have shown that the Markov processes approach can be applied to the description of the turbulent cascade in the fast solar wind. The Chapman-Kolmogorov equation is approximately satisfied in the inertial range, as well as for larger scales up to $\tau=86\,400$ s. Numerical solution of the Fokker-Planck equation agrees well with experimental probability distributions obtained directly from the data in the

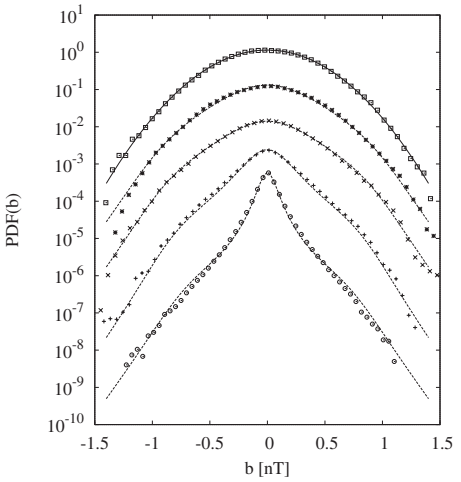

FIG. 6. Experimental probability distributions (points) and solution of the Fokker-Planck equation (dashed lines) for initial condition (solid line) obtained by approximation of the experimental PDF by Gaussian distribution for $\tau=86\,400$ s. We show the comparison of the experimental PDF and solution of Eq. (7) for τ equal to 86 400, 30 000, 5000, 1000, 100 s (from the top). Probability distributions for different scales have been shifted in the vertical direction for clarity of presentation.

range of τ from 100 to 86 400 s. Therefore, we can conclude that for intermittent solar wind turbulence, the Markov processes approach can provide a mathematical formalism capable of explaining the specific evolution of the shape of the probability distribution with scale changing from the energy containing scale down to the dissipation scale. Since the formalism describes properly the evolution of the probability distribution with scale, obviously this should also work for structure functions, which are defined as appropriate moments of the probability distributions. Admittedly, direct analytical derivation of the scaling properties of the structure functions can be difficult, but we expect that such studies can be done numerically. As we noticed in the Introduction, the Markov processes approach has been tested for hydrodynamical turbulence in a number of papers, confirming its Markovian character. Therefore, the results of our analysis of solar wind turbulence confirm the universality of the Markov processes approach to the description of turbulent cascades in general. One should also notice that there is a theoretical interest in the application of conditional probability distributions (and structure functions) to the description of turbulent cascades [25,26].

In our opinion, the observed Markovian character is related to the universal character of large-scale instabilities, which are fundamental physical mechanisms involved in the generation of turbulence. One of the most fundamental assumptions in the studies of turbulence is that in the fully developed case (large Reynolds numbers) the turbulent cascade in the inertial range has universal structure and properties, i.e., the properties are assumed to be independent of details of the force driving the turbulent flow [10]. Given this assumption, the transfer of fluctuations to smaller scales must be independent of the dynamics on large scales (which are past scales from the point of view of a turbulent cascade), because otherwise the structure of the process being the driver of turbulence would be transferred toward smaller scales, and no universal structure of the dynamics in the inertial range would have been observed. This tendency of turbulent flows to form universal cascades (universal character of large-scale instabilities) provides a fundamental physical explanation for the observed Markovian (which physically means "memoryless") character of solar wind turbulence. Therefore, our results provide evidence that the transfer of fluctuations in solar wind turbulence is really "memoryless," and that we should expect a universal structure in the turbulent dynamics.

Every Markov process must satisfy the Chapman-Kolmogorov equation, which expresses the condition that the probability density of the transition from the scale τ_2 to τ_1 can be subdivided into smaller steps, that is, the transition from the scale τ_2 to τ', and then from the scale τ' to τ_1. Therefore, in the case of a turbulent cascade, fulfillment of the Chapman-Kolmogorov equation can be interpreted as the presence of a local transfer mechanism in scales, and consequently in the wave vector space, providing that the Taylor hypothesis is satisfied. Local and nonlocal transfer mechanisms can be distinguished in theoretical studies of turbulence via shell models or numerical simulations (see, e.g., [27–29]), but it is very difficult to study the property of turbulence using experimental data. The Markov processes approach seems to provide such a method. Namely, analyzing a time series from a turbulent flow we should be able to identify the character of the dominating transfer mechanism for a given quantity or between different quantities, i.e., we should be able to answer the question of whether the mechanism is local or nonlocal.

Therefore, another physical consequence of the Markovian property is the local character of the transfer mechanism of fluctuations in solar wind turbulence. In general, the question of locality of the energy transfer in magnetohydrodynamic turbulence is not well understood and quite complicated because of the strong influence of the mean magnetic field on small-scale plasma dynamics. The question of locality of the energy transfer is of some interest, e.g., in the studies of the dynamo mechanism to generate magnetic fields in astrophysical objects, where in helical MHD turbulence, nonlocal processes of generation of large-scale fields by small-scale helicities are studied in detail (see, e.g., Sec. 6.2.1 of [11]). The question is also important for modeling MHD flows and numerical simulations, e.g., in large-eddy simulations, where low-pass filtering with respect to a cutoff wave number requires some assumptions concerning the transfer of energy around the cutoff wave number.

Since our results suggest rather the Markovian character of the turbulent cascade in the solar wind, it indicates that the local transfer mechanism dominates in solar wind turbulence. Therefore dominating transfer of magnetic field fluctuations has similar character as in the case of Kolmogorov phenomenology describing turbulence in neutral fluids, where according to the picture of Richardson cascade, the energy transfer has local character in the wave vector space,

i.e., the energy at a scale l is transferred mainly to smaller but comparable scales [10]. This result is somewhat surprising, because we analyze here magnetohydrodynamic turbulence, which is rather a magnetic field dominated case. Therefore, according to the classical Iroshnikov-Kraichnan picture, due to the Alfvén effect, we could expect nonlocal influence of large-scale magnetic field on small-scale turbulent eddies, and so also nonlocal interactions between modes [11]. Nevertheless, results of recent numerical simulations suggest that local transfer mechanisms dominate in MHD turbulence [27–29]. Our paper provides experimental results confirming this observation for magnetic-to-magnetic transfer of fluctuations.

ACKNOWLEDGMENTS

We would like to thank the Ulysses Data System and the Principal Investigator, A. Balogh of Imperial College, London, UK for magnetic field data. This work has been supported by the Polish Ministry of Science and Higher Education through Grant No. N N202 4127 33.

[1] W. H. Matthaeus and M. L. Goldstein, J. Geophys. Res. **87**, 6011 (1982).
[2] M. L. Goldstein, D. A. Roberts, and W. H. Matthaeus, Annu. Rev. Astron. Astrophys. **33**, 283 (1995).
[3] C.-Y. Tu and E. Marsch, Space Sci. Rev. **73**, 1 (1995).
[4] M. L. Goldstein and D. A. Roberts, Phys. Plasmas **6**, 4154 (1999).
[5] E. Marsch and C. Y. Tu, Ann. Geophys. **12**, 1127 (1994).
[6] L. Sorriso-Valvo, V. Carbone, P. Veltri, G. Consolini, and R. Bruno, Geophys. Res. Lett. **26**, 1801 (1999).
[7] L. Sorriso-Valvo, V. Carbone, P. Giuliani, P. Veltri, R. Bruno, V. Antoni, and E. Martines, Planet. Space Sci. **49**, 1193 (2001).
[8] L. F. Burlaga, J. Geophys. Res. **106**, 15917 (2001).
[9] R. Bruno and V. Carbone, Living Rev. Solar Phys. **2**, 4 (2005).
[10] U. Frisch, *Turbulence: The Legacy of A. N. Kolmogorov* (Cambridge University Press, Cambridge, 1995).
[11] D. Biskamp, *Magnetohydrodynamic Turbulence* (Cambridge University Press, Cambridge, 2003).
[12] G. Pedrizzetti and E. A. Novikov, J. Fluid Mech. **280**, 69 (1994).
[13] R. Friedrich and J. Peinke, Physica D **102**, 147 (1997).
[14] R. Friedrich and J. Peinke, Phys. Rev. Lett. **78**, 863 (1997).
[15] J. Davoudi and M. R. Tabar, Phys. Rev. Lett. **82**, 1680 (1999).
[16] C. Renner, J. Peinke, and R. Friedrich, J. Fluid Mech. **433**, 383 (2001).
[17] C. Renner, J. Peinke, R. Friedrich, O. Chanal, and B. Chabaud, Phys. Rev. Lett. **89**, 124502 (2002).
[18] B. Hnat, S. C. Chapman, and G. Rowlands, Phys. Rev. E **67**, 056404 (2003).
[19] R. Schwenn, Space Sci. Rev. **124**, 51 (2006).
[20] K. P. Wenzel, R. G. Marsden, D. E. Page, and E. J. Smith, Astron. Astrophys. Suppl. Ser. **92**, 207 (1992).
[21] A. Balogh, T. J. Beek, R. J. Forsyth, P. C. Hedgecock, R. J. Marquedant, E. Smith, D. J. Southwood, and B. T. Tsurutani, Astron. Astrophys. Suppl. Ser. **92**, 221 (1992).
[22] E. J. Smith, B. V. Connor, and G. T. Foster, Jr., IEEE Trans. Magn. **11**, 962 (1975).
[23] P. C. Hedgecock, Space Sci. Instrum. **1**, 61 (1975).
[24] H. Risken, *The Fokker-Planck Equation: Methods of Solution and Applications*, 2nd ed., Springer Series in Synergetics (Springer, Berlin, 1989).
[25] V. L'vov and I. Procaccia, Phys. Rev. Lett. **76**, 2898 (1996).
[26] V. S. L'vov and I. Procaccia, Phys. Rev. E **62**, 8037 (2000).
[27] O. Debliquy, M. K. Verma, and D. Carati, Phys. Plasmas **12**, 042309 (2005).
[28] A. Alexakis, P. D. Mininni, and A. Pouquet, Phys. Rev. E **72**, 046301 (2005).
[29] P. Mininni, A. Alexakis, and A. Pouquet, Phys. Rev. E **72**, 046302 (2005).